Monitoring Production Process of Cisplatin-Loaded PLGA Nanoparticles by FT-IR Microspectroscopy and Univariate Data Analysis

Marianna Portaccio,[1,2] Ciro Menale,[1,2,3] Nadia Diano,[1,2] Carla Serri,[4] Damiano G. Mita,[2,3] Maria Lepore[1,2]

[1]Dipartimento di Medicina Sperimentale – Seconda Università di Napoli, Napoli, Italy
[2]Consorzio Interuniversitario INBB, Rome, Italy
[3]Istituto di Genetica e Biofisica "A. Buzzati Traverso" CNR, Napoli, Italy
[4]Dipartimento di Scienze Biol. Ambientali, Università degli Studi di Messina, Messina, Italy
Correspondence to: M. Lepore (E-mail: m.lepore@unina2.it)

ABSTRACT: Cisplatin-loaded PLGA nanoparticles for drug delivery have been prepared using a well-established water/oil/water double emulsion-solvent evaporation method. The production process has been monitored by using Fourier Transform Infrared (FT-IR) microspectroscopy without using KBr tablets and any preliminary sample preparation. Significant spectra have been obtained for all chemical compounds and for samples at different steps of production process. The use of a linear or univariate approach using a R^2 determination coefficient has been proposed for discriminating among FT-IR spectra even when small differences are present. The obtained results confirm that new geometries of data acquisition contribute to make infrared microspectroscopy a very useful tool for a rapid and detailed monitoring of production processes of pharmacological interest. Moreover, morphological and physiological characterizations have been performed on cisplatin-loded samples showing results in good agreement with those reported in literature. © 2014 Wiley Periodicals, Inc. J. Appl. Polym. Sci. **2015**, *132*, 41305.

INTRODUCTION

In recent years, biodegradable polymer nanoparticles have received considerable attention for drug delivery with the aim to improve their bio-availability preserving the therapeutic efficacy. One of the most investigated system is represented by cisplatin-loaded poly-(D, L-lactic-*co*-glycolic)acid (PLGA) nanoparticles.[1,2] PLGA is one of the best materials in terms of prevention of premature drug degradation, side effects reduction, drug efficacy enhancement, and achievement of requested drug release rates. To enhance the effectiveness of PLGA as a potential drug carrier, several methods have been established in order to obtain high drug encapsulation efficiency, controlled drug release, and desired particle sizes and configurations.[3–10] Different experimental techniques have been used to monitor these preparation methods. For example, for determining particle size, size distribution and morphology dynamic light scattering (DLS), scanning and transmission electron microscopy, and atomic force microscopy have been adopted.[11–14] Among the different experimental techniques generally used for analysing surface chemistry of cisplatin-loaded PLGA nanoparticles Fourier Transform Infrared (FT-IR) microspectroscopy has been used together with X-ray photoelectron

microscopy and nuclear magnetic resonance spectroscopy.[15–18] In particular, FT-IR microspectroscopy can play a specific role owing to its capability in identifying chemical groups in heterogeneous compounds.[15] By analysing the features of a recorded infrared spectrum, the composition or the structure of chemical components can be determined.[16] In almost all the reported FT-IR studies, spectra of cisplatin loaded-PLGA nanoparticles have been obtained by using KBr pellets and conventional transmission geometry acquisition.[19–22] The use of KBr even though not particularly complex sometimes can be time consuming and requires that personnel involved in measurements is exposed to toxic products during tablets preparation. To avoid this undesirable step FT-IR microscopy in reflection geometry can be very useful. In such a way, spectra can be directly collected without any particular sample preparation, measurements result nondestructive (or slightly destructive) and spectra can be acquired from the same sample at different times.

The aim of the present paper is to report on micro FT-IR measurements performed at each step of nanoparticle preparation to evidence the contribution of different compounds. For this purpose, cisplatin-loaded PLGA nanoparticles have been prepared

using a well-established water/oil/water double emulsion-solvent evaporation method. An univariate analysis procedure has been proposed for interpreting experimental results when the spectrum modifications are relatively weak.[23–25] In this case, it can be difficult to quantitatively evaluate the effect of possible changes in state or configuration on small spectral regions, because of the presence of noise, background or spurious signals. A global analysis of the spectrum can provide some advantages in the evaluation of spectral changes, especially when the spectra to be compared have a close configuration. Linear regression analysis in FT-IR has been already adopted for chemical imaging study, for quantitative purposes in spectroscopic analysis, for providing a measure of similarity between data sets, for distinguishing polymorphs and for two-dimensional correlation spectroscopy.[24,26–31] In the present case, the use of this procedure has enabled us to discriminate the presence of small quantities of cisplatin in PLGA nanoparticles.

Morphological and physiological characterizations have also been performed on the prepared sample for confirming the effectiveness of PLGA as a potential drug carrier.

EXPERIMENTAL

Materials
Poly(D,L-lactic-co-glicolic)acid (PLGA), cis-diammineplatinum(II)dichloride (Cis-Pt), Polyvinyl Alcohol (PVA) (average molecular weight 30,000–70,000), N,N-Dimethylformamide (DMF), o-phenilenediamine (o-PDA), and chloroform were purchased from Sigma-Aldrich (St. Louis, MO, USA). All chemical were used as received without any further purification. Culture media (DMEM, RPMI-1640, and Ham's-F10) and fetal bovine serum (FBS) were obtained from Euroclone (Milan, Italy).

Nanoparticle Preparation
PLGA nanoparticles (NPs) were prepared by a water/oil/water (w/o/w) double emulsion-solvent evaporation method from a copolymer (lactide : glicolide = 50 : 50) having molecular weight 40.000–75.000.[32] Briefly, 2 mL of 25% DMF aqueous solution were added dropwise to 5 mL of chloroform containing 150 mg of PLGA and emulsified using a probe sonicator (Soniprep 150, Sanyo MSE, London, UK) at 10 Amplitude microns for 5 min in an ice bath. This first emulsion (w/o) was added to 18 mL of 1% (w/v) PVA aqueous solution to obtain the second emulsion (w/o/w) sonicating as for the first emulsion. To allow chloroform evaporation, the resulting emulsion was continuously stirred, overnight and at room temperature, on a magnetic stirrer plate. The obtained nanoparticles were collected by three cycles of centrifugation at $10,000 \times g$ for 10 min, washed three times with water and afterward lyophilized for 24 hr. The nanoparticles are stored at $-20°C$ until use.

Cisplatin loaded nanoparticles (Cis-Pt NPs) were prepared following the same protocol but adding 10 mg of cisplatin to the aqueous solution containing DMF. For monitoring nanoparticle preparation procedure samples after each step were properly stored until use and air-dried before FT-IR measurements.

Nanoparticle Morphological Characterization
Nanoparticle morphology was examined by Transmission Electronic Microscopy (TEM, Leica Microsystem, Germany) sus-

pending nanoparticle preparation in 2% (v/v) phosphotungstic acid solution. Z-Potential, particle size and Poly Dispersion Index (PDI) were measured using Zetasizer Nano Series and Dynamic Light Scattering (Malvern Instruments, UK) after resuspension of nanoparticle formulation in 1 mL of phosphate buffered saline (PBS, pH 7.4).

Determination of Cisplatin Content
Cisplatin content was estimated using a modified colorimetric assay.[33] Five milligrams of Cis-Pt NPs were dissolved in 0.5 mL of DMF and the solution was mixed with the same volume of 1.4 mg/mL o-PDA dissolved in DMF. The mix solution was heated at 90°C for 30 min in a waterbath then it was placed in ice for 10 min to block the reaction. The same procedure was performed with 5 mg of NPs used as blank. The reaction solution was transferred into a poly(methyl-methacrylate) cuvette for absorbance measurements in an UV-VIS spectrophotometer (PerkinElmer Massachusetts, USA) at 720 nm.

Loading Efficiency (LE) and Encapsulation Efficiency (EE) were calculated according to Jin et al.:[34]

$$\text{Loading efficiency (LE\%)} = \frac{\text{Amount of drug in nanoparticles}}{\text{Amount of drug loaded nanoparticles}}, \quad (1)$$

$$\text{Encapsulation efficiency (EE\%)} = \frac{\text{Amount of drug innanoparticles}}{\text{Initial amount of drug}}. \quad (2)$$

The measurements were performed in triplicate and the evaluated parameters are expressed as the mean of the three replicates ±SD.

FT-IR Microspectroscopy
Data Acquisition. A Perkin Elmer Spectrum One FT-IR spectrometer equipped with a Perkin Elmer Multiscope system infrared microscope (Mercury Cadmium Telluride detector (MCT)) was used to record FT-IR spectra. Spectral acquisitions were performed in specular-reflection mode with thin layers of sample put on a metallic IR-reflective surface. The background spectrum was collected from the metallic IR-reflective surface in the absence of the sample. A sampling spot on the surface was selected through an objective (10X optical or 15X infrared). All spectra were collected using 16 scans in the range from 4,000 to 600 cm^{-1} with a 4 cm^{-1} spectral resolution. The spectra were preliminarily analyzed using the application routines provided by the software package ("Spectrum" User Guide, Perkin Elmer Inc. USA) controlling the whole data acquisition system. "Spectrum" (release 5.0.2, 2004) is the main Perkin Elmer software package for collecting, viewing and processing IR spectra.

Univariate Data Analysis. As said before, univariate analysis is largely used in FT-IR spectroscopy with different purposes. One of the most useful applications concerns the comparison between two spectra for estimating the similarity between them as in the present case. To this aim, different statistical univariate parameters can be adopted.[25] In our case for each wavenumber point, the intensity of the spectrum (y_i variable) is compared with the corresponding value of another spectrum variable (x_i variable), referring to the sample in different condition. In order

Table I. Characteristics of PLGA Nanoparticles Obtained from TEM, DLS, and ζ-Potential Measurements[a]

	NPs	NPs-CisPt
Particle Size by TEM (nm)	198 ± 15	197 ± 16
Particle Size by DLS (nm)	197 ± 5	195 ± 2
ζ-potential (mV)	−18.4 ± 0.7	−20.2 ± 0.5
PDI	0.013	0.042
LE (%)		8.2 ± 1.2
EE (%)		47.1 ± 5.3

[a] LE and EE parameters were evaluated as defined in Ref. 34. The measurements were performed in triplicate and the evaluated parameters are expressed as the mean of the three replicates ±SD.

to overcome constraints related to the possible different scale of the experimental data, the data set is directly correlated with a linear scaling of the other signal. This means to do a linear regression or univariate analysis of data. The basic assumption is that the spectrum Y (containing the n data y_i) is a linear function of another spectrum X (containing the n data x_i). All variations with respect to the X signal are considered as a perturbation term ε_i:

$$Y_i = mx_i + p + \varepsilon_i, \tag{3}$$

If no structural change occurs in the substance generating the spectra, the term ε_i depends only on the experimental conditions and we can assume that it has random values that follow a Gaussian distribution, with mean 0 and variance σ_y. Regression analysis allows to determine, by means of a least square fit of data y_i with respect to x_i, the parameters m and p and to identify the linear dependence. A useful parameter to check how well a regression equation fits the data is the sample coefficient of determination, R^2.[24,25] It is defined as:

$$R^2 = 1 - \frac{\Sigma[y_i - (mx_i + p)]^2}{\Sigma[y_i - \bar{y}]^2}, \tag{4}$$

where $\bar{y}$ is the average value of vector Y. R^2 ranges from 0 for uncorrelated data, to 1 for perfect linear dependence. When the error ε is purely random, the value of R^2 is equivalent to the square of the covariance $r_{y\hat{y}}$, calculated for the vector Y and the prediction vector $\hat{Y}$ having components $\hat{y}_i = mx_i + p$, which is defined as: [24,25]

$$r_{y\hat{y}} = \frac{\Sigma(y_i - \bar{y})(\hat{y}_i - \bar{\hat{y}})}{[\Sigma(y_i - \bar{y})^2]^{1/2}[\Sigma(\hat{y}_i - \bar{\hat{y}})^2]^{1/2}}, \tag{5}$$

R^2 is thus an index of the correlation between the considered set of data and the linear dependence on the reference signal, as we have postulated. The linear regression was evaluated on a number of points ranging between 500 and 700. Due to the high number of points considered, the values reported for R^2 in the next paragraph imply a high level of significance.

Assay of Swelling Degree
Particle mean diameter was measured as previously described after resuspension of nanoparticle formulation in 1 mL of the appropriate solution. To investigate the effect of pH on swelling degree, nanoparticles were dissolved in PBS solution at different

pH values (2.0, 4.0, 6.0, 7.4, and 10). To study the effect of physiological fluids on swelling degree, the experiments were performed using three different cell culture media (RPMI-1640, DMEM and HAM's-F10) supplemented with 10% Fetal Bovine Serum (FBS) at 37°C (±1°C). Double Distilled Water (DDW) was used as control. The percentage of swelling degree (Sw %) as calculated as:

$$Sw\% = \frac{D_{a,f} - D_{a,i}}{D_{a,i}} 100\% \tag{6}$$

where $D_{a,f}$ and $D_{a,i}$ are the average final and initial nanoparticle diameter, respectively. The measurements were performed in triplicate.

In Vitro Release
Drug release analysis from PLGA nanoparticles was carried out in PBS, pH 7.4. Ten milligram of cisplatin-loaded nanoparticles were added to 0.5 mL of PBS and placed in an orbital shaker at 120 rpm at 37°C. At prefixed time intervals, up to 340 hr, the solution was centrifuged at 10,000 × g for 10 min. The surnatant was recovered to quantify the amount of released cisplatin. The precipitated nanoparticles were resuspended in 0.5 mL fresh PBS and replaced on the shaker. The amount of cisplatin recovered at each measure was added to the previous recorded value.

RESULTS AND DISCUSSION

Nanoparticle Morphological Characterization
The results of particle size, PDI and the ζ-Potential measurements are reported in Table I and expressed as the mean of three replicates ±SD. It is interesting to note that no differences results in the nanoparticle sizing using TEM or DLS measurement techniques that provide measures consistent with each other within experimental error. Also worthy of mention is that the value of the ζ-potential, which mediates the dispersion between the nanoparticles and their interaction with cellular membrane, is similar to that reported by other authors.[32] This means also that particles are resuspended in a stable solution and that they do not form aggregates. No statistical differences are found between loaded and unloaded nanoparticles in the size, ζ-potential and PDI. All these characteristics are maintained during the time (data not shown). Particles shape and size are important parameters for drug release and for bioavailability since well rounded nanometric particles are better internalized in the tumour sites.[35] The prepared nanoparticles have the expected spherical form as well as a good dispersion. In Figure 1, the TEM images of the nanoparticle preparation loaded (1a) or unloaded (1b) with cisplatin are shown. It is clear that the two preparations have a similar appearance in agreement also with the results reported in literature.[36]

Determination of Cisplatin Content
LE and EE parameters are obtained using Eqs. (1) and (2) and a calibration curve (with a linear range equal to 1–200 µg/mL and slope equal to 0.0019 ± 0.0001 mL/µg) for the quantification of cisplatin dissolved in DMF. Their values are also shown in Table I and are similar to the ones reported in literature.[2,32]

FT-IR Measurements
FT-IR Spectra of Chemicals. The pure PVA sample IR spectrum is reported in Figure 2 and exhibits typical bands for vinyl
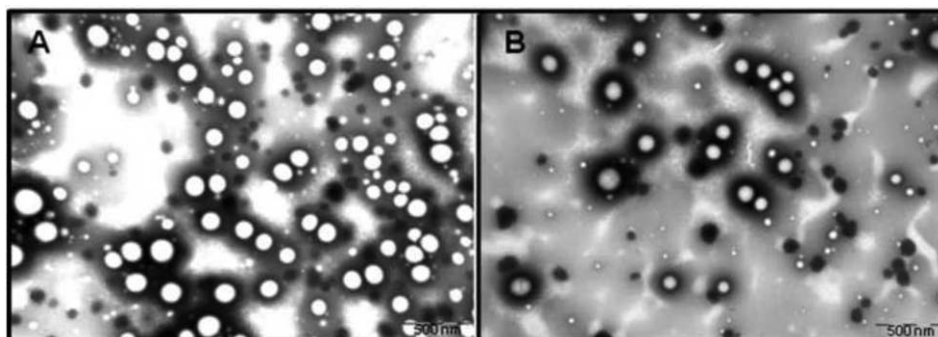
Figure 1. Representative TEM images of PLGA nanoparticles formulated with w/o/w double emulsion solvent evaporation method. (a) Cis-Pt-loaded nanoparticles and (b) Empty nanoparticles. Magnification 50,000X. Scale bar corresponds to 500 nm.

synthetic polymers. In particular, the spectrum shows a broad hydroxyl band at 3355 cm^{-1}, a C–H stretching vibration peak from alkyl groups at 2942 cm^{-1}, a C=O stretching peak at 1735 cm^{-1}, a C=C stretching peak at 1651 cm^{-1}. Contributions from CH bending of alkanes and CH and OH bending are evinced at 1432 cm^{-1} and 1375 cm^{-1}, respectively. Moreover, peaks at 1251 cm^{-1} (C–C–O stretching), 1092 cm^{-1} (O–C–C stretching) and 946 cm^{-1} (OH bending) are evident. The presence of certain amount of carbonyl groups arises from the production process of PVA, which is obtained from poly (vinyl acetate) by hydrolysis.[37,38] Thus, there is always a small content of residual acetate groups.[39,40] See Table II for peak positions and assignments. For comparison also the PVA chemical structure is reported.

In Figure 3, the PLGA spectrum is shown. In this spectrum, the peaks due to asymmetric stretching vibrations of CH$_3$ and CH$_2$ are located at 2996 cm^{-1} and 2948 cm^{-1}, respectively. The contribution of carbonyl-C=O stretching vibration is strongly present at 1773 cm^{-1}. Other less intense peaks are present at 1453 cm^{-1} (CH$_3$ bending), at 1424 cm^{-1} (C–H bending of glycolic acid O–CH$_2$ and OH in plane bending), at 1394 cm^{-1} (CH$_3$ bending), and at 1272 (cm^{-1} C–O stretching of carboxylic acid). An intense peak is located at 1176 cm^{-1} due to C–C–O

stretching from ester group. Also an intense contribution from O–C–C stretching from ester is observed at 1098 cm^{-1}. Moreover, a very small shoulder at 956 cm^{-1} (OH bending) is present. See Table III for chemical structure and for a complete list of peak positions and assignments.[20–22]

In Figure 4, the FT-IR spectrum of DMF is reported. The band assignments for DMF have already been reported in the literature.[41–43] In the present case, the CH$_3$ symmetric stretching mode is observed at 2943 cm^{-1}, CH stretching mode at 2862 cm^{-1}, C=O stretching mode at 1660 cm^{-1}, CN stretching mode at 1506 cm^{-1}, CH$_3$ asymmetric bending mode at 1438 cm^{-1}, N–C–H bending mode at 1387 cm^{-1}, CN asymmetric stretching at 1255 cm^{-1}, CH$_3$ rocking mode at 1091 and

Table II. Chemical Structure of PVA[a]

PVA chemical structure
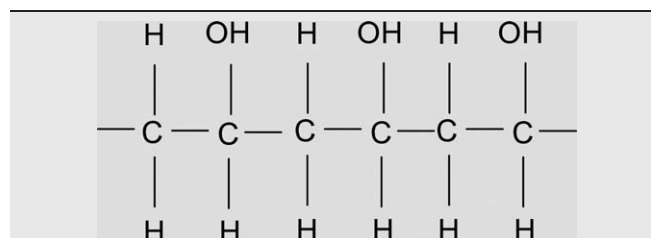
Wavenumber (cm^{-1})	Assignment
3355	OH stretching
2942	CH stretch of alkanes
1735*	C=O stretching
1651*	C=C stretching
1432	CH bending of alkanes
1375	CH and OH bending
1251*	C-C–O stretching
1092*	O-C-C stretching
946	OH bending
846	No assignment is available

[a] Main peaks in the FT-IR spectrum of PVA samples and tentative assignment according to Refs. 39-42. In particular, peaks with asterisk are due to the production process, PVA chains can contain acetate groups which did not undergo hydrolysis in the production process of polyvinyl alcohol from polyvinyl acetate according to Refs. 39,40.
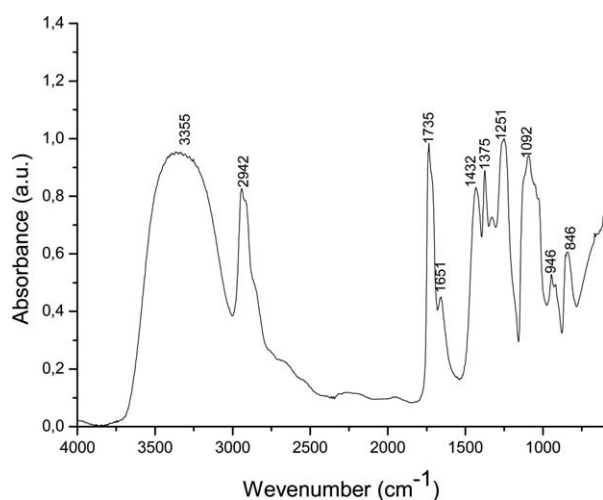

Figure 2. PVA representative FT-IR spectrum with main peaks wavenumber positions.
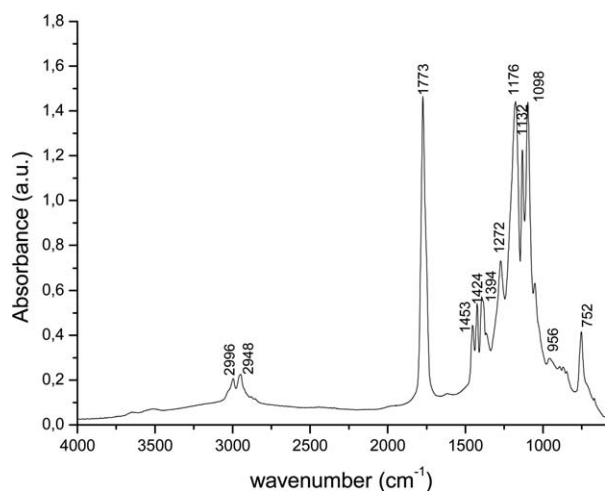
Figure 3. PLGA representative FT-IR spectrum with main peaks wavenumber positions.

Figure 4. DMF representative FT-IR spectrum with main peaks wavenumber positions

1061 cm^{-1}, CN symmetric stretching at 863 cm^{-1} and the O=C–N stretching mode at 657 cm^{-1}. For further details about chemical structure and peak assignments see Table IV.

As far as concern Cis-Pt characteristics in Table VI, the chemical structure and the main peaks present in IR spectrum are reported together with their assignments.[44–46] We avoided to use pure Cis-Pt in FT-IR equipment to avoid possible contamination.

FT-IR Monitoring of Nanparticle Preparation Procedure. In Figure 5, results from FT-IR monitoring of each step of nanoparticle preparation are reported. For comparison, all the spec-

tra are normalized with respect to the highest peak in the spectra that is related to the C=O stretching. To better clarify the spectrum modifications occurring during the subsequent phases of nanoparticle preparation (from Figure 5(a–e)), the FT-IR spectrum of pure PLGA (Figure 5a) is also reported. In Figure 5b, spectrum from PLGA/DMF w/o emulsion sample is reported. The presence of a new peak at 1674 cm^{-1} clearly shows the presence of a carbonyl group (C=O) due to the contribution of DMF (see Table IV). The addition of PVA to the first emulsion produces in the spectrum of the previous phase peaks typical of polyvinylalcohol as can be seen from Figure 5c

Table III. Chemical Structure of PLGA[a]

PLGA chemical structure

Wavenumber (cm^{-1})	Assignment
2996	Asymmetric stretching CH$_3$
2948	Asymmetric stretching CH$_2$
1773	Carbonyl —C=O stretcthing
1453	C—H bending of CH$_3$
1424	CH bending of O—CH$_2$ (of glycolic acid) and OH in plane bending
1394	C—H bending of CH$_3$
1272	C—O stretching of carboxylic acid
1176	C—C—O stretching from ester
1132	No assignment is available
1098	O—C—C stretching from ester
956	OH bending

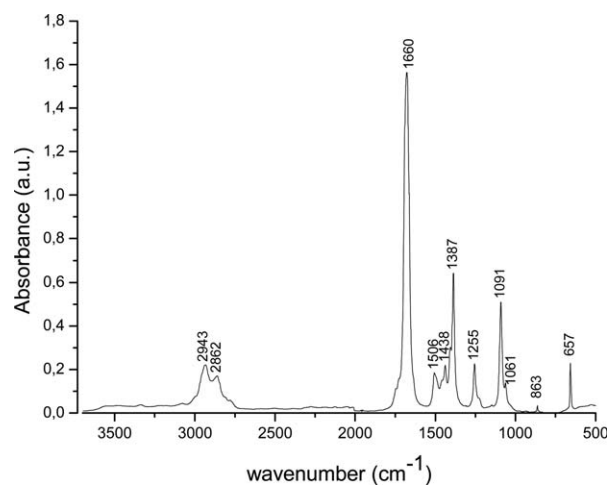[a] Main peaks in the FT-IR spectrum of PLGA samples and tentative assignment according to refs. 20-22.

Table IV. Chemical Structure of DMF[a]

DMF chemical structure

Wavenumber (cm^{-1})	Assignment
2943	CH asymmetric stretching of alkanes
2862	CH symmetric stretching of alkanes
1660	C=O stretching
1506	CN stretching
1438	CH asymmetric bending
1387	N—C—H bending
1255	CN asymmetric stretching
1091–1061	CH rocking mode
863	CN symmetric stretching
657	O=C—N stretching

[a] Main peaks in the FT-IR spectrum of DMF samples and tentative assignment according to refs. 43–45.
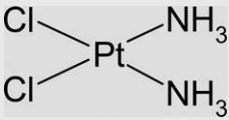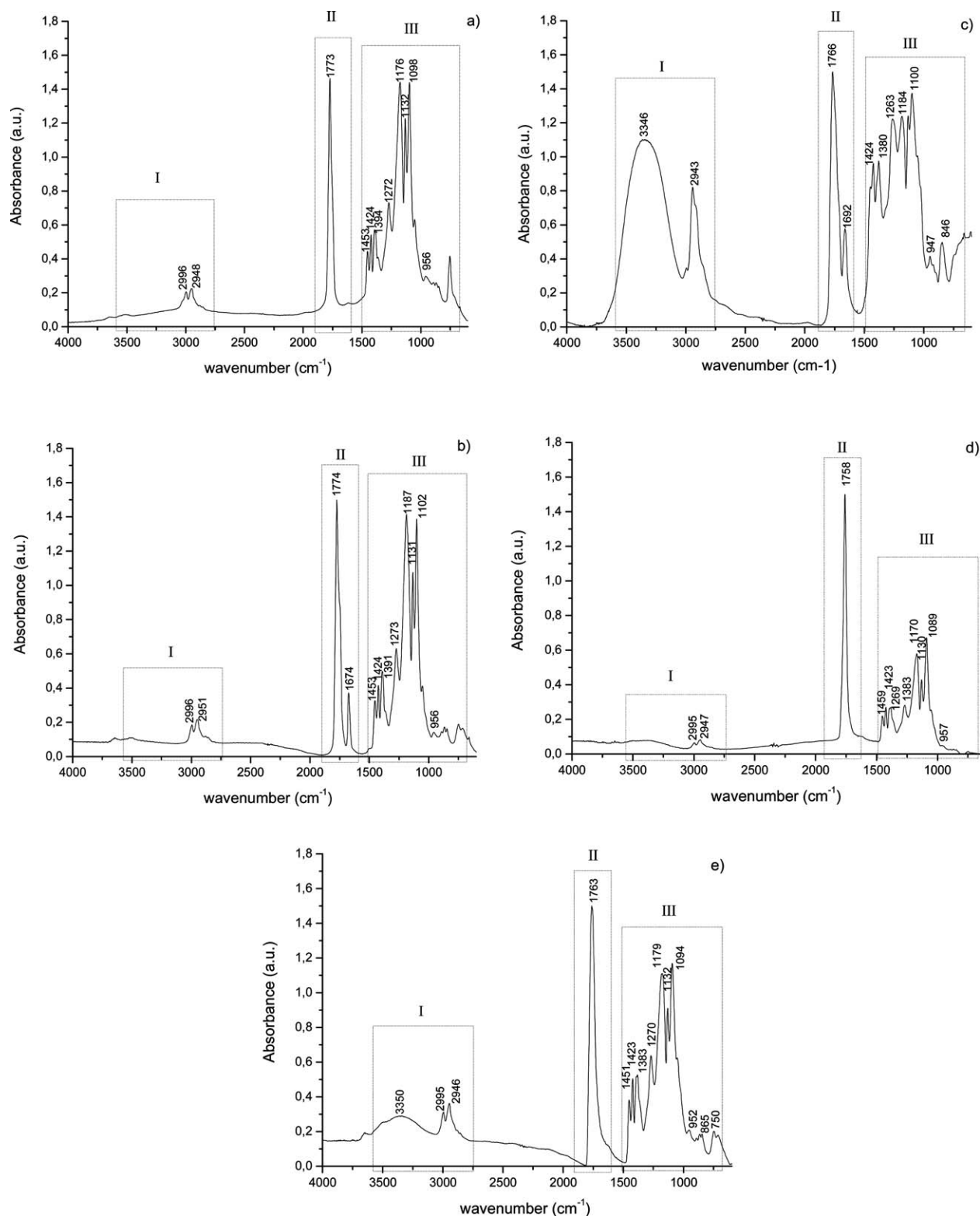
Figure 5. Representative FT-IR spectra of samples from different procedure steps: (a) pure PLGA sample; (b) PLGA with DMF addition (1° emulsion); (c) sample of 1° emulsion after PVA addition (2° emulsion); (d) samples after washing procedure; and (e) sample with Cis-Pt added.

(PLGA/DMF/PVA sample w/o/w emulsion). In particular, in Region I (2800–3800 cm^{-1}) peaks of stretching of OH (3346 cm^{-1}) are evident together with those of stretching of

CH introduced by PVA. In Region II (1900–1600 cm^{-1}), a peak can be seen at 1766 cm^{-1} that is given by the convolution of contribution of carbonyl from emulsion w/o at 1773 cm^{-1} and

Table V. Chemical Structure of Cis-Pt

Cis-Pt chemical structure	
Cl—Pt(—NH₃)(—NH₃)—Cl	
Wavenumber (cm⁻¹)	Assignment
3297	NH asymmetric stretching
3232	NH symmetric stretching
1625	NHN asymmetric bending
1544	NHN asymmetric bending
1316	NHN symmetric bending
1301	NHN symmetric bending
795	HNH in-plane bending

Main peaks in the FT-IR spectrum of Cis-Pt and tentative assignment from Refs. 46–48.

the peak at 1735 cm^{-1} of the PVA. Similarly, also in the region III (1500–650 cm^{-1}) several peaks due to the superimposition of the spectrum of the first emulsion and of PVA are noticed. In Figure 5d, the FT-IR representative spectrum of a PLGA/DMF/PVA nanoparticle sample is reported after washing. As is evident PVA contribution is almost disappeared confirming that the removal procedure has been successful. In Figure 5e, the FT-IR spectrum of the sample after the addition of Cis-Pt is also reported. Changes are expected in the 3300–3200 cm^{-1} (related to asymmetric and symmetric stretching of NH group), 1600–1300 cm^{-1} (related to HNH asymmetric and symmetric bending) region and around 800 cm^{-1} (related to HNH in plane bending. See Table V for further details.[46–48] As is evident an increase is present in these regions when Figure 5e is compared to Figure 5d but we did not find significant new peaks that can be directly related to Cis-Pt infrared spectra. This situation is not unusual, in fact notwithstanding the large number of papers related to Cis-Pt loaded PLGA nanoparticles only very few experimental IR evidences of Cis-Pt presence are reported.[47]

Univariate Analysis of Cis-Pt Content. When spectrum modifications are relatively weak and not characterized by the appearance of new peaks a global analysis of the spectrum can provide some advantages in the evaluation of spectral changes, especially when the spectra to be compared have a close configuration. As in this case, only a new component has been added to samples. As said before, several correlation methods have been typically employed in these situations in order to enhance similarities or correlation in the data sets.[23,24,48] In Figure 6, the results of our univariate data analysis are reported. Spectra of different samples of nanoparticles with and without Cis-Pt have been considered and the different R^2 values have been plotted. In particular, on the axes the file numbers are reported. Numbers from 1 to 4 refer to spectra of Cis-Pt NP samples, while numbers from 5 to 8 are related to spectra of NP without Cis-Pt. As is evident when the R^2 parameter is evaluated between two spectra related to samples with the same chemical composition its value is significantly higher (R^2 ranging between 0.99 and 0.8) than the one calculated between spectra related to samples with different

chemical composition (R^2 ranging between 0.6 and 0.3). These results confirm that the use of the R^2 parameter can be very useful for evaluating experimental results when no clear evidence of new peaks is obtained and only weak changes are present between spectra. Moreover, in the present case the R^2 values can be directly related to the presence or absence of Cis-Pt. In fact, the addition of this element is the only difference occurring between samples examined with univariate analysis.

The FT-IR microspectroscopy measurements demonstrate the validity of the chosen production process of cisplatin-loaded PLGA nanoparticles. In order to complete our study, we report the results of physiological characterizations to confirm the potential of these nanoparticles as drug carrier.

pH Effects on Nanoparticle Swelling Degree
Changes in nanoparticle swelling were evaluated by using Eq. (6) at different pH conditions of the PBS solution in which the nanoparticles were suspended. The results are reported in Figure 7a and indicate that after 24 hr PLGA nanoparticles show maximum swelling degree at physiological pH solution (pH 7.4), while nanoparticles have a lower swelling degree in acidic and alkaline conditions. It is worthy to mention that at extremely acidic pH (pH 2.0) no size values can be detected since the *in vitro* biodegradation/hydrolysis of PLGA in strongly acidic media accelerates polymer erosion, while under slightly acidic or alkaline media conditions the swelling degree is less marked due to autocatalysis by the PLGA carboxylic end groups.[49]

Physiological Fluid Effects on Nanoparticle Swelling Degree
To study the effects of different biological solutions on PLGA nanoparticle swelling degree, the size analysis was performed by dissolving the preparation in three typical cell culture media widely used to culture different cell lines depending on their nutritional needs. In particular, RPMI-1640, DMEM, and HAM's-F10, all supplemented with 10% FBS. As said before double distilled water was used as control. These culture media were used to simulate conditions in which the different
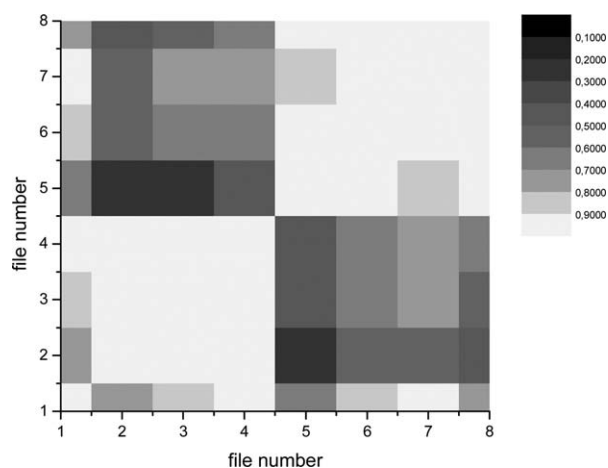

Figure 6. R^2 determination coefficient (95% confidence level) resulting from the linear regression of infrared spectra related to loaded and unloaded nanoparticles. Axis labels indicate the file numbers. Numbers from 1 to 4 refer to spectra of Cis-Pt NP samples, while numbers from 5 to 8 are related to spectra of NP without Cis-Pt.

composition of the media can influence the swelling behavior. In Figure 7b, the swelling degree is reported for each of the different cell culture media and DDW after 24 hr. It is clear that the swelling degree depends on the media composition. Since all the solutions used in the experiments contained the same amount of serum, the swelling effects are largely due to the different amount and nature of additives present in the media. DMEM-high glucose (containing glucose, amino acids, and vitamins with concentration higher than other media) produces lower extent of swelling degree of PLGA nanoparticles as occurs for DDW. Compared to other basal media, HAM's-F10 contains a wider variety of components, including zinc, hypoxanthine, and thymidine while RPMI-1640 is characterized by the reducing agent glutathione, biotin, and high concentrations of vitamins. The presence of such additives increased the swelling degree compared to the other solutions.

In Vitro Kinetic Drug Release

Our previous study has shown that the *in vitro* kinetics release has a linear triphasic trend. The first phase is characterized by an initial and rapid linear burst release for the first 3 hr related to the delivery of the cisplatin adsorbed on the external nanoparticle surface. The second one lasting up to 4 days is another linear phase characterized by a lower constant release rate. Finally, a third linear phase exhibiting the lowest release rate

Table VI. Cisplatin Release Kinetic Values[a]

Release phases	$y_i(0)$ (μg)*	k_i (μg/h)*
Phase 1	0.00	8.92
Phase 2	32.65	0.16
Phase 3	45.28	0.04

[a] $y_i(0)$: cisplatin concentration at the beginning of each phase; k_i: release constant rate.

lasting up to 14 days was observed. At the end of the three phases, the cisplatin release reaches about 80% of the total encapsulated cisplatin. The resulted profile was very similar to that reported by other studies[50] where the release of different compounds encapsulated in PLGA particles was analyzed.

Each one of the three release phase is expressed by the general equation:

$$y_i(t) = y_i(0) + k_i t, \qquad (7)$$

where i indicates the different phases (1, 2, 3); $y_i(t)$ represents the amount in micrograms of released cisplatin at the time t and $y_i(0)$ is the cisplatin concentration value at the beginning of each phase. t is the time measured in hr and k_i represents the release constant rate expressed in micrograms /hr. In Table VI, the $y_i(0)$ and the k_i values evaluated for each of the three phases are listed.

CONCLUSIONS

In this paper, FT-IR microspectroscopy has been used to monitor the production process of Cis-Pt-loaded PLGA nanoparticles for drug delivery without using KBr tablets and any preliminary sample preparation so avoiding the unnecessary manipulation of toxic products. The spectra here reported have allowed us to clearly characterize the different steps of the used nanoparticle production process. Moreover, the use of a linear or univariate approach using a R^2 determination coefficient for discriminating among FT-IR spectra even when small differences are present has been employed and it has been proven useful to evidence the Cis-Pt presence in spectra with subtle differences. The obtained results confirm once more that infrared microspectroscopy can be usefully adopted for a rapid and detailed monitoring of production processes of pharmacological interest. Moreover, the usefulness of PLGA nanoparticles as drug carrier model system has been demonstrated by characterizing samples from physiological point of view. In particular, pH and physiological fluid effects on nanoparticle swelling degree have been evaluated together with *in vitro* kinetic drug release.

Figure 7. Effect of different pH (a) and different biological fluids (b) on PLGA nanoparticle swelling degree.

REFERENCES

1. Marques, M. P. M.; ISRN Spectroscopy **2013** Article ID 287353 http://dx.doi.org/10.1155/2013/287353.

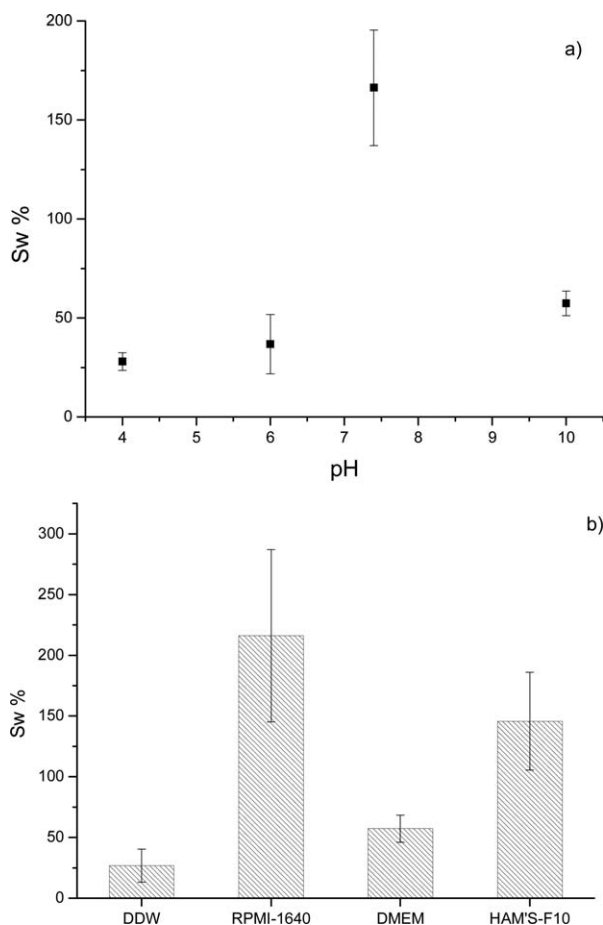2. Dinarvand, R.; Sepehri, N.; Manoochehri, S.; Rouhani, H.; Atyabi, F. *Int. J. Nanomedicine* **2011**, *6*, 877.

3. Dong, Y.; Feng, S. S. *Int. J. Pharm.* **2007**, *342*, 208.

4. Cartiera, M. S.; Johnson, K. M.; Rajendran, V.; Caplan, M. J.; Saltzman, W. M. *Biomaterials* **2009**, *30*, 2790.

5. Tahara, K.; Sakai, T.; Yamamoto, H.; Takeuchi, H.; Hirashima, N.; Kawashima, Y. *Int. J. Pharm.* **2009**, *382*, 198.

6. Zolnik, B. S.; Burgess, D. J. *J. Control Release* **2008**, *127*, 137.

7. Grama, C. N.; Ankola, D. D.; Kumar, M. N. V. R. *Curr. Opin. Colloid. Interface Sci.* **2011**, *16*, 238.

8. Bala, I.; Hariharan, S.; Kumar, M. N. *Crit. Rev. Ther. Drug. Carrier Syst.* **2004**, *21*, 387.

9. Shive, M. S.; Anderson, J. M. *Adv. Drug Deliv. Rev.* **1997**, *28*, 5.

10. Kumari, A.; Yadav, S. K.; Yadav, S. C. *Colloids Surf. B* **2010**, *75*, 1.

11. Cheng, F. Y.; Wang, S. P.; Su, C. H.; Tsai, T. L.; Wu, P. C.; Shieh, D. B.; Chen, J. H.; Hsieh, P. C.; Yeh, C. S. *Biomaterials* **2008**, *29*, 2104.

12. Esmaeili, F.; Ghahremani, M. H.; Ostad, S. N.; Atyabi, F.; Seyedabadi, M.; Malekshahi, M. R.; Amini, M.; Dinarvand, R. *J. Drug Target* **2008**, *16*, 415.

13. Panyam, J.; Sahoo, S.; Prabha, S.; Bargar, T.; Labhasetwar, V. *Int. J. Pharm.* **2003**, *262*, 1.

14. Ravi Kumar, M.; Bakowsky, U.; Lehr, C. *Biomaterials* **2004**, *25*, 1771.

15. Gunzler, H.; Gremlich, H. U. IR Spectroscopy; Wiley-VCH: Weinheim, **2002**.

16. Gremlich, H. U.; Yan, B. Infrared and Raman Spectroscopy of Biological Materials; Marcel Dekker: New York, **2001**.

17. Si-Shen, F.; Li, M.; Guofeng, H. *Curr. Med. Chem.* **2004**, *11*, 413.

18. Chenga, J.; Teplya, B. A.; Sherifia, I.; Sunga, J.; Luthera, G.; Gu, F. X.; Levy-Nissenbauma, E.; Radovic-Morenob, A. F.; Langera, R.; Farokhzad, O. C. *Biomaterials* **2007**, *28*, 869.

19. Yang, J.; Hwan Lee, C.; Park, J.; Seo, S.; Lim, E. K.; Song, Y. J.; Suh, J. S.; Yoon, H. G.; Huh, Y. M.; Haam, S. *J. Mater. Chem.* **2007**, *17*, 2695.

20. Matsumoto, A.; Matsukawa, Y.; Suzuki, T.; Yoshino, H.; Kobayashi, M. *J. Control Release* **1997**, *48*, 19.

21. Gryparis, E. C.; Mattheolabakis, G.; Bikiaris, D.; Avgoustakis, K. *Drug Deliv.* **2007**, *14*, 371.

22. Fu, K.; Griebenow, K.; Hsieh, L.; Klibanov, A. M.; Langer, R. *J. Control Release* **1999**, *58*, 357.

23. Asuero, A. G.; Sayago, A.; González, A. G. *Crit. Rev. Anal. Chem.* **2006**, *36*, 41.

24. Blanco, M.; Cruz, J.; Bautista, M. *Anal. Bioanal. Chem.* **2008**, *392*, 1367.

25. Taylor, J. R. An Introduction to Error Analysis, The Studies of Uncertainties in Physical Measurements, Universities Science Books: Sausalito, USA, **1982**.

26. Jovanovic, N.; Gerich, A.; Bouchard, A.; Jiskoot, W. *Pharm. Res.* **2006**, *23*, 2002.

27. Li, D.; Sedman, J.; García-González, D. L.; van de Voort, F. R. *J. ASTM Int.* **2009**, *6*, Paper ID JAI102110.

28. Szakonyi, G.; Zelko, R. *J. Pharm. Biomed. Anal.* **2012**, *63*, 106.

29. Moes, J. J.; Ruijken, M. M.; Gout, E.; Frijlink, H. W.; Ugwoke, M. I. *Int. J. Pharm.* **2008**, *357*, 108.

30. Patel, A. D.; Luner, P. E.; Kemper, M. S. *J. Pharm. Sci.* **2001**, *90*, 360.

31. Peng, Y.; Wu, P. *Polymer* **2004**, *45*, 5295.

32. Moreno, D.; de Ilarduya, C. T.; Bandres, E.; Bunuales, M.; Azcona, M.; Garcia-Foncillas, J.; Garrido, M. *J. Eur. J. Pharm. Biopharm.* **2008**, *68*, 503.

33. Taylor, A.; Krupskaya, Y.; Krämer, K.; Füssel, S.; Klingeler, R.; Büchner, B.; Wirth, M. P. *Carbon* **2010**, *48*, 2327.

34. Jin, C.; Bai, L.; Wu, H.; Song, W.; Guo, G.; Dou, K. *Pharm. Res.* **2009**, *26*, 1776.

35. Gao, Y.; Chen, L.; Gu, W.; Xi, Y.; Lin, L.; Li, Y. *Mol. Pharm.* **2008**, *5*, 1044.

36. Cohen-Sela, E.; Chorny, M.; Koroukhov, N.; Danenberg, H. D.; Golomb, G. *J. Control Release* **2009**, *133*, 90.

37. Majumdar, S.; Adhikari, B. *Sens. Actuators B* **2006**, *114*, 747.

38. Mansur, H. S.; Sadahira, C. M.; Souza, A. N.; Mansur, A. A. P. *Mater. Sci. Eng. C* **2008**, *28*, 539.

39. Labidi, N. S.; Djebali, A. *J. Miner. Mater. Character. Eng.*, **2008**, *7*, 147.

40. Ilčin, M.; Holá, O.; Bakajová, B.; Kučerík, J. *J. Radioanal. Nucl. Chem.* **2010**, *283*, 9.

41. Jacob, M. M. E.; Arof, A. K. *Electrochim. Acta* **2000**, *45*, 1701.

42. Jao, T. C.; Scott, I. *J. Mol. Spectrosc.* **1982**, *92*, 1.

43. Stalhandske, C. M. V.; Mink, J.; Sandstrom, M.; Papai, I.; Johnsson, P. *Vib. Spectrosc.* **1997**, *14*, 207.

44. Ye, Q. S.; Liu, W. P.; Chen, X. Z.; Yu, Y.; Chang, Q. W.; Hou, S. Q. *Arch. Pharm. Res.* **2010**, *33*, 807.

45. Amado, A. M.; Fiuza, S. M.; Marques, M. P. M.; Batista de Carvalho, L. A. E. *J. Chem. Phys.* **2007**, *127*, Article ID 185104.

46. de Carvalho, L. A. E. B.; Marques, M. P. M.; Martin, C.; Parker, S. F.; Tomkinson, *J. Chem. Phys. Chem.* **2011**, *12*, 1334.

47. Yan, X.; Gemeinhart, R. A. *J. Control Release* **2005**, *106*, 198.

48. Camerlingo, C.; Delfino, I.; Perna, G.; Capozzi, V.; Lepore, M. *Sensors* **2011**, *11*, 8309.

49. Makadia, H. K.; Siegel, S. *J. Polymers-Basel* **2011**, *3*, 1377.

50. Avgoustakis, K.; Beletsi, A.; Panagi, Z.; Klepetsanis, P.; Karydas, A. G.; Ithakissios, D. S. P. L. *J. Control Release* **2002**, *79*, 123.